日本原子力研究開発機構機関リポジトリ

Japan Atomic Energy Agency Institutional Repository

Japan Atomic Energy Agency

Investigation of potential conjugate adsorbent for efficient ultra–trace gold(III) detection and recovery

Md. Rabiul Awual *

Actinide Coordination Chemistry Group, Quantum Beam Science Directorate (QuBS), Japan Atomic Energy Agency (SPring–8), Hyogo 679–5148, Japan

* Corresponding author. Tel.: +81–791–58–2642; fax: +81–791–58–0311.
E–mail address: awual75@yahoo.com, awual.rabiul@jaea.go.jp (M. R. Awual).

Research highlights:

➢ Conjugate adsorbent is prepared for simultaneous ultra–trace Au(III) ion capturing.

➢ Adsorbent can selectively detect the Au(III) in presence of diverse competing ions.

➢ Adsorbent has high stability and reusability without deterioration in Au(III) capturing.

Graphical Abstract
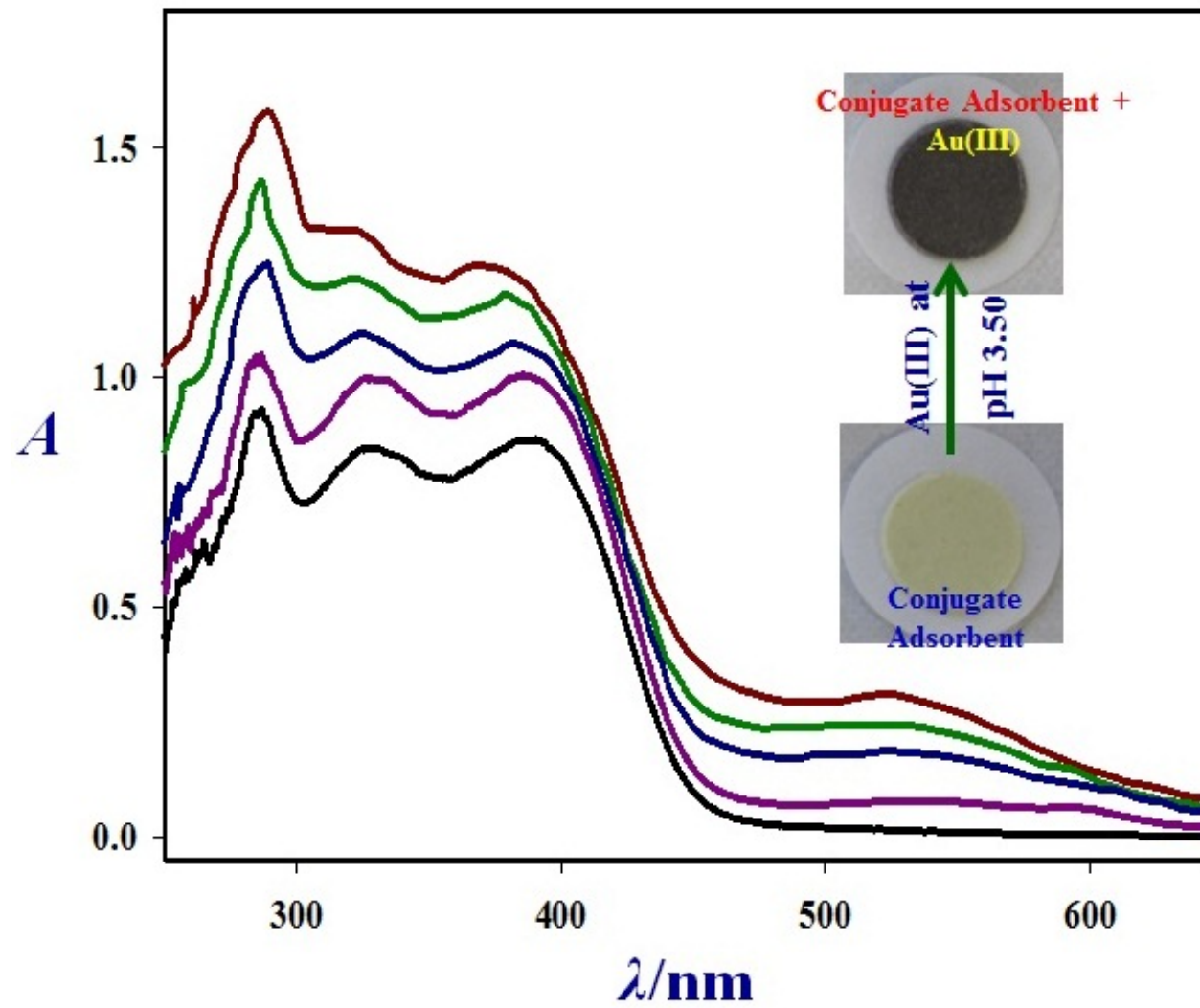
A B S T R A C T

A novel conjugate adsorbent was developed for simultaneous Au(III) detection and recovery from urban mining waste. This adsorbent has the large surface area–to–volume ratios and uniformly shaped pores in the nanostructures in its cage cavities. Therefore, the conjugate adsorbent permitted to fast and specific Au(III) ions capturing via a colorimetric naked–eye visualization based on stable complexation [Au(III)–DHDM]$^{n+}$ mechanism. The detection limit and sorption capacity of the novel adsorbent at optimum conditions was 0.22 µg/L and 183.42 mg/g, respectively. The design in such novel adsorbent offered a simple procedure for ultra–trace Au(III) detection and recover without using highly sophisticated instruments.

Keywords: Ultra–trace Au(III); Conjugate adsorbent; Detection and recovery; Sensitivity and selectivity; Reuses.

1. Introduction

Gold (Au(III)) is one of the most precious metals due to its usage and application in different areas such as jewelry, high–tech industries, and electronic apparatus [1–4]. Moreover, Au(III) possesses unique properties in physical and chemical that promote its widespread industrial applications. Therefore, the recovery of Au(III) is an attracting challenge due to the limited sources and growing industrial demand [5,6]. The determination and recovery of Au(III) are often restricted owing to interferences of the high concentration of interfering matrix components and insufficient selectivity and selectivity of different adsorbents to ultra–trace level of Au(III) ions in environmental, geological and metallurgical samples [7,8]. In order to solve the problems of economic impact of losing Au(III) and environmental concern, it is important to develop simple, efficient, environment–friendly, selective and rapid methods for determination and recovery of Au(III) by suitable materials.

Determination of ultra–trace Au(III) ions in waste samples with inexpensive methods is one of the principal challenges that scientists are facing. Many methods have been reported to detect the Au(III) ions such as inductively coupled plasma mass spectrometry (ICP–MS), ICP–OES, electrothermal atomic absorption spectrometry (ETAAS), flame atomic absorption spectrometry (FAAS) and spectrophotometry [8–13]. The ICP–MS and ICP–AES/OES are more sensitive instruments and able to detect very low level Au(III) ions. However, these sophisticated instruments and complicated sample preparation hampers their application for in–field studies [7]. Therefore, interest in innovative methods to determine the Au(III) in waste scraps has been increasing based on simple, robust, cost–effective, easy–to–use and efficient sensitivity. Then an effective method for technological diversity is the optical ligand immobilized conjugate materials model based on generating the analytical signal as a response to binding with Au(III) ions has drawn great attention as effective devices to full–fill such a requirement.

Several methods have been applied to separate and recover of Au(III) ion from waste such as ion exchange, membrane separation, coprecipitation, solvent extraction, cloud point extraction and sorption on a solid phase by different functional groups activity for ion exchange or stable complexation mechanism [14–24]. The presence of specific functional groups in solid materials is needed for complexation with Au(III) ions based selectivity and sensitivity [7,25]. However, the solution acidity playing an important role to bind trace level Au(III) to these functional groups. Moreover, the sorption of a solute on a solid support has the advantage over solvent extraction in that no excessive slugged are produced and considered as environment–friendly technology and effective for ultra–trace Au(III) recovery from urban mining waste samples [7]. In this connection, our focus is now towards developing various functional materials for specific metal ions detection and recovery from a

variety of urban mining and environmental samples, as they are cheap and environmental friendly.

The nanaomaterials based nanotechnology is growing considerable public interest for ultra–trace metal ions capturing due to the high surface–area–to–volume ratio makes them suitable method [26,27]. The specific ligands incorporated from these inorganic silica materials have drawn the considerable attention due to active functionality of the organic ligand with thermal and mechanical stabilities in specific metal ions in solution buffer solution activity. However, the conventional ligands are slow metal–ion capturing and lack of selectivity toward a particular metal ion [28,29]. Then the specific and fast complexation of the metal ions with ligand immobilized conjugate adsorbent was investigated for selective and sensitive detection and recovery of Au(III) ions from waste scrap.

In this study, highly selective ligand of *N,N*(octane–1,8–diylidene)di(2–hydroxy–3,5–dimethylaniline) (DHDM) was successfully immobilized onto inorganic mesoporous silica and then examined as a new class conjugate adsorbent for ultra–trace Au(III) detection and recovery of Au(III) ions from urban mining waste. The DHDM onto inorganic mesoporous silica was associated based on non–covalent interactions, Van der Waals forces and reversible covalent bonds. Moreover, the mesoporous silica exhibited high ordered nanostructure, in which the pores were well arranged and homogeneous as nanocage structure with large pore volume to use as an excellent carrier for the producing of ligand incorporated conjugate adsorbent for detection and recovery of Au(III). This work describes a simple and efficient conjugate adsorbent preparation with an immobilizing ligand functionalization for Au(III) recovery systems. The experimental studies were carried out by batch approaches. The influence of various parameters such as solution acidity, color optimization, limit of detection, Au(III) sorption capacity, competing ions effects and Au(III) recovery behaviour were systematically investigated and discussed. A complete laboratory investigation of this

process would generally consist of three parts such as (i) preparation of conjugate adsorbent, (ii) demonstration of detection operation and feasibility low detection limit and (iii) optimum sorption operation to obtain data to be used in designing the full–scale plant.

2. Materials and methods

2.1. Materials

All materials and chemicals were of analytical grade and used as purchased without further purification. Tetramethylorthosilicate (TMOS), the triblock copolymers of poly(ethylene oxide–b–propylene oxide–b–ethylene oxide) designated as F108 ($EO_{141}PO_{44}EO_{141}$) and 1,8–Octanediol were obtained from Sigma–Aldrich Company Ltd. USA. The standard Au(III) ions solutions, and metal salts for the source of metal ions were purchased from Wako Pure Chemicals, Osaka, Japan. For pH adjustments in optical detection, buffer solutions of 3–morpholinopropane sulfonic acid (MOPS), 2–(cyclohexylamino) ethane sulfonic acid (CHES) and *N*–cyclohexyl–3–aminopropane sulfonic acids (CAPS) were procured from Dojindo Chemicals, Japan, and KCl, HCl, NaOH from Wako Pure Chemicals, Osaka, Japan. Ultra–pure water prepared with a Millipore Elix Advant 3 was used throughout in this work.

2.2. Synthesis and characterization of DHDM ligand

The structure and preparation of the *N*,*N'*–(octane–1,8–diylidene)di(2–hydroxy–3,5–dimethylaniline) (DHDM) is shown in **Scheme 1**. The DHDM was prepared by the reaction of 1,8–Octanediol (one moles) and 2–hydroxy–3,5–dimethylaniline (two mole) in ethanol and small amount of acetic acid was added. The resultant mixture was then heated under reflux for 4 h and left to cool at room temperature. The solid formed upon cooling was collected by suction filtration. The separated product was recrystallized using dichloromethane/methanol

6

1/1. Then the purpose materials were dried at 50°C for 24 h. The purity of the DHDM was analyzed by CHN elemental analyses. The observed values ($C_{24}H_{34}N_2O_2$) were C, 75.32%; H, 8.88%; N, 7.31% and the calculated values were C, 75.39%; H, 8.90%; N, 7.33%. The product was characterized by ^1H NMR spectroscopy. The ^1H NMR (400 MHz, CDCl$_3$): δ 1.29 (H, methylene), 1.52 (H, methylene), 2.15 (H, methyl), 2.34 (H, methyl), 5.34 (H, aromatic C–OH), 6.92 (H, benzene), 7.12 (H, benzene), 7.50 (H, aldimine). ^{13}C NMR (400 MHz, CDCl$_3$): δ 15.4 (CH, CH$_3$), 21.6 (CH, CH$_3$), 26.3 (CH, CH$_2$), 28.6 (CH, CH$_2$), 29.1 (CH, CH$_2$), 122.2 (CH, benzene), 129.3 (CH, benzene), 130.8 (CH, benzene), 132.2 (CH, benzene), 136.8 (CH, benzene), 149.1 (CH, benzene), 163.7 (CH, C–iminie).

2.3. Synthesis of inorganic mesoporous silica monoliths

The surfactant of F108 (EO$_{141}$PO$_{44}$EO$_{141}$, MW: 14,600) was used as scaffolds in preparation of mesoporous inorganic silica monoliths. The mesoporous inorganic silica materials procedure involved adding of TMOS and triblock copolymers (F108) to obtain a homogenized sol–gel mixture based on the F108/TMOS mass ratio. An acidified aqueous solution was added to the mixture to quickly achieve the desired liquid–crystal phase and then to promote hydrolysis of the TMOS around the liquid–crystal phase assembly of the triblock copolymer surfactants. However, the preparation was methods reported elsewhere [28]. However, the composition mass ratio of F108:TMOS:HCl/H$_2$O was 1.4:2:1 respectively. Homogeneous sol–gel synthesis was achieved by mixing F108/TMOS in a 200 mL beaker and then shaking at 55–60°C until homogeneous. The exothermic hydrolysis and condensation of TMOS occurred rapidly by addition of acidified aqueous HCl acid (at pH = 1.3) solution to this homogeneous solution. The methanol produced from the TMOS hydrolysis was removed by using a diaphragm vacuum pump connected to a rotary evaporator at 45°C. The organic moieties were then removed by calcination at 500°C for 6 h

under the normal atmosphere. After that, the inorganic silica was grounded properly and ready to use for direct immobilization with synthesized DHDM ligand to prepare as new class conjugate adsorbent for selective determination and recovery of Au(III) ions.

2.4. Preparation of new class conjugate adsorbent

The conjugate adsorbent was prepared by direct immobilization of DHDM in ethanol solution 50 mg into 1.0 g inorganic mesoporous silica. The immobilization procedure was performed under vacuum at 35°C for 6 h stirring until DHDM ligand saturation was achieved. The ethanol was removed by a vacuum connected to a rotary evaporator at 45°C and the resulting conjugate adsorbent was washed with warm water to check the stability and elution of DHDM from inorganic mesoporous silica. The DHDM exhibited of specific functional groups for actively bonding to Au(III) ions in detection and sorption operations by a stable complexation mechanism because the DHDM incorporated with inorganic mesoporous silica by abundant hydroxyl groups of pore surface silicates and the heteroatoms of DHDM organic ligand. Then the material was dried at 60°C for 5 h and grounded into fine powder for Au(III) detection and recovery experiments. The DHDM immobilization amount (0.09 mmol/g) was determined by the following equation:

$$Q = (C_0 - C)\ V/m \tag{1}$$

where Q is the adsorbed amount (mmol/g), V is the solution volume (L), m is the mass of inorganic silica materials (g), C_0 and C are the initial concentration and supernatant concentration of the DHDM, respectively.

2.5. Au(III) ions recognition

In recognition system, the conjugate adsorbent was immersed in a mixture of specific Au(III) ions concentrations (2.0 mg/L) and adjusted at appropriate pH of 1.01, 2.01, 3.0 (0.2 M of KCl with HCl), 5.20 (0.2 M CH$_3$COOHCH$_3$COONa with HCl) and 7.01 (MOPS with NaOH) in the specific amount of the adsorbent (8 mg) at constant volume (10 mL) with shaking in a temperature–controlled water bath with a mechanical shaker at 25°C for 10 min at a constant agitation speed of 110 rpm to achieve good color separation. In addition, the blank solution was also prepared, following the same procedure for comparison of optimum color formation. After color optimization, the solid materials were filtered using Whatman filter paper (25 mm; Shibata filter holder) and used for color assessment and absorbance measurements by solid–state UV–Vis–NIR spectrophotometer for the qualitative and quantitative estimation of Au(III) ions. The low of detection limit (L_D) of Au(III) ions was determined from the linear part of the calibration plot according to the following equation [27]:

$$L_D = KS_b/m \tag{2}$$

where, K value is 3, S_b is the standard deviation for the blank and m the slope of the calibration graph in the linear range, respectively.

2.6. Au(III) sorption, recovery and reversibility

In sorption systems, the conjugate adsorbent was also immersed in Au(III) ions concentrations and adjusted at specific pH values by adding of HCl or NaOH in 20 mL solutions for 1 h at room temperature and amount of adsorbent was also used of 8 mg. Then the adsorbent was separated by filtration system and Au(III) concentrations in before and after sorption operations were analyzed by ICP–AES. The batch sorption experiments were performed at room temperature (25°C). The amount of adsorbed Au(III) was calculated according to the following equations:

$$\text{Mass balance } q_e = (C_0 - C_f) \; V/M \text{ (mg/g)} \tag{3}$$

$$\text{and Au(III) sorption efficiency } Re = \frac{(C_0 - C_f)}{C_0} \times 100 \; (\%) \tag{4}$$

where V is the volume of the aqueous solution (L), and M is the weight of the conjugate adsorbent (g), C_0 and C_f are the initial and supernatant Au(III) ions concentrations in solutions, respectively.

In recovery/extraction operation, first 20 mL of 2.5 mM Au(III) ion solution was adsorbed by the 20 mg adsorbent and then recovery/extraction experiments were performed using different concentrations of H_2SO_4, HCl, and HCl–thiourea solutions. The adsorbed Au(III) metal ions onto conjugate adsorbent was washed with deionized water several times and transferred into 50 mL beaker. To this 5 mL of the stripping agent was added, and then the solutions were stirred for 10 min. The concentration of Au(III) ion released from the adsorbent into aqueous phase was analyzed by ICP–AES. Also, the conjugate adsorbent was reused several cycles to investigate the reusability. All experiments in this study were duplicated to assure the consistency and reproducibility of the results.

2.7. Analyses

The N_2 adsorption–desorption isotherms were measured using BELSORP MINI–II analyzer (JP. BEL Co. Ltd.) at 77 K. The pore size distribution was measured from adsorption isotherms plot by using nonlocal density functional theory (NLDFT). The inorganic silica material was pre–treated at 100°C for 3 h under vacuum until the pressure was equilibrated to 10^{-3} Torr before the N_2 isothermal analysis. The specific surface area (S_{BET}) was measured by using multi–point adsorption data from linear segment of the N_2 adsorption isotherms using Brunauer–Emmett–Teller (BET) theory. The NMR spectra was

obtained on a Varian NMR System 400 MHz Spectrometer. Transmission electron microscopy (TEM) was obtained by using a JEOL (JEM–2100F) and operated at the accelerating voltage of the electron beam 200 kV. The TEM samples were prepared by dispersing the powder particles in ethanol solution using an ultrasonic bath and then dropped on copper grids. The absorbance spectrum was measured by UV–Vis–NIR spectrophotometer (Shimadzu, 3700). The metals ion concentrations were measured by ICP–AES (SII NanoTechnology Inc.). The ICP–AES instrument was calibrated using five standard solutions containing 0, 0.5, 1.0, 1.5 and 2.0 mg/L (for each element), and the correlation coefficient of the calibration curve was higher than 0.9999. In addition, sample solutions having complicated matrices were not used and no significant interference of matrices was observed.

3. Results and discussion

3.1. Inorganic mesoporous silica and conjugate adsorbent

The N_2 isotherms show the typical IV type adsorption behavior with a broad H_2 type hysteresis loop and well–defined steepness of isotherms well–known sharp inflection of adsorption/desorption branches (**Fig. 1**) and adsorption branches were significantly shifted toward lower relative pressure (P/P_0) indicated that uniform cagelike pore structures were characteristic of the silica monoliths [**26**]. However, this kind of isotherms is complying of super–microporous materials that have a pore size between the micro– and mesopore domains [**30,31**]. In this synthetic design, the mesoporous silica exhibited the appreciable textural parameters of mesopore volume (Vp), specific surface area (S_{BET}), and tunable pore diameters. The large pore volume, pore diameter, and high surface area of mesoporous silica evident that the materials have mesoporous structure in its case cavities. Therefore, the mesoporous silica has great advantages for preparing of ligand incorporated conjugate adsorbent to detect and recovery of ultra–trace Au(III) ions from urban mining waste. In

addition, the stability of the conjugate adsorbent was confirmed by strong electrostatic interactions between heteroatoms of DHDM ligand molecule and charged inorganic mesoporous silica.

The scanning electron microscopy images of as–synthesized samples are typical of mesoporous silica and show large particle morphologies (**Fig. 2 (A, B)**). The macropores size also evidents the higher magnification SEM image in the range from 1 to 10 µm. The TEM images showed a well arrangement pores and continuous arrays along all directions (**Fig. 2(C, D)**) which indicate the direct interaction between the DHDM and inorganic silica into the rigid condensed pore surfaces with retention of the ordered structures, leading to high flux and Au(III) ion transport during detection and sorption processes. In addition, the TEM image exhibited well–organized parallel channels and clarified a hexagonally ordered array in the direction parallel to the pore which clarified the prepared material has a typical hexagonal [**29**].

The conjugate adsorbent was fabricated by direct immobilization method. After immobilization of DHDM, a decrease in the surface area (S_{BET}) and average pore diameter of conjugate adsorbent provided further the presence of DHDM ligand to the surface partially blocks the adsorption of nitrogen molecules as judged from **Fig. 1**(b); however, a significant amount might also anchor on the outer surfaces of the cage. The materials characterization also confirmed that the ability to achieve flexibility in the specific activity of the electron acceptor or donor strength of the chemically responsive DHDM ligand molecule may lead to easy generation and transduction of visual color signal in the naked–eye detection and sorption of ultra–trace Au(III) ions by a stable complexation mechanism with specific selectivity. It was confirmed that the cage character was maintained even after incorporated of the ligand molecules onto mesoporous silica. Then the wide–range functionalities of the optical conjugate adsorbent make the detection and recovery systems technologically

promising from the practical view point.

3.2. Au(III) ions detection parameters

The solution acidity is playing an important role in the selective detection of Au(III) ions by using proposed conjugate adsorbent. The effect of pH of the aqueous solution employing the buffer solutions on the detection of the developed colored complex ion associate was studied by measuring the absorbance intensity. The reflectance spectra of the Au(III)–adsorbent complexes on pore surfaces was evaluated over a wide range of solution pH (**Fig. 3**) based on the acceptor–donor combinations between Au(III) and DHDM ligand on the conjugate adsorbent. The absorbance spectra of $[Au(III)–DHDM]^{n+}$ complex at $\lambda = 390$ nm was carefully investigated to obtain the specific pH region for maximum absorbance intensity. Results showed that the optimal conditions in the reaction of Au(III) with DHDM was in an acid medium. The maximum absorbance of the produced ion associate was obtained at pH 3.50. However, the color signalling of Au(III) ions by the conjugate adsorbent is mainly dependent on the stable complexation of Au(III)–DHDM binding at the specific pH conditions [**28**]. Therefore, the pH 3.50 was chosen as optimum experimental condition in accordance with sensitivity and selectivity, and the rest of the detection experiment was performed at pH 3.50 in this study.

The color intensity measurement by UV–Vis–NIR absorption spectroscopy of conjugate adsorbent in solid showed a strong $[Au(III)–DHDM]^{n+}$ by charge–transfer (intense π–π transition) band at 390 nm by the addition of Au(III) ions at pH 3.50. The reflectance absorbance spectral intensity increased with increasing Au(III) concentration from 0.002 to 2.0 ppm as shown in **Fig. 4(A)**. The reflectance spectra was observed at λ_{max} of 390 nm as a result of complexation and the signaling detection of Au(III) ions with the DHDM ligand of the conjugate adsorbent surface. In this study, the color change provided a simple procedure

for the sensitive detection of Au(III) ions without using of highly sophisticated instruments. Therefore, the sensitive Au(III) detection at ultra–trace concentrations by optical naked–eye observation indicated the high performance of the conjugate adsorbent.

The low limit of detection of Au(III) ions for the conjugate adsorbent was estimated from the linear part of the calibration plot of the absorbance spectra of the [Au(III)–DHDM]$^{n+}$complex at 390 nm against the Au(III) ion concentration. The calibration plots of the conjugate adsorbent show a linear correlation at low concentration of Au(III) ions as shown in **Fig. 4(B)**. A linear correlation in the range from 0.01 to 0.508 µM was observed (**Fig. 4(B)** inset). At higher concentration over 0.508 µM, the dependence is nonlinear due to saturation effects, indicating that sensitive detection of low concentrations of Au(III) ions. The resultant low of limit detection value (0.22 µg/L) indicated that the conjugate adsorbent enabled Au(III) detection of ultra–trace Au(III) ions, even in the presence of the several matrices (calibration curve with dotted lines). Therefore, the conjugate adsorbent can effectively separate and preconcentrate the Au(III) ions even at trace concentrations.

The ion selectivity of the conjugate adsorbent is crucial due to several interfering ions and species are co–existed in waste scraps [**5,7,9**]. Then the Au(III) selectivity of the conjugate adsorbent was evaluated at optimum detection conditions. In this evaluation, the competing ions (Zn^{2+}, Fe^{3+}, Bi^{3+}, Pt^{2+}, Ru^{3+}, Ag^+, Ni^{2+}, Cu^{2+} and Co^{2+}) concentration was 5–folds higher than the Au(III) ion concentration. These ions were considered to interfere if it resulted in a ±5% variation of the absorbance intensity compared with blank sample. The color profiles and absorbance spectra after the addition of competing ions signals responses in accordance with reflectance spectra are depicted in **Fig. 5**. The data clarified that the diverse competing ions did not show any considerable spectral change compared with blank sample except Au(III) ions. The results indicated that conjugate adsorbent has high selectivity

to Au(III) ions due to strong tendency to form stable complexation with DHDM ligand of conjugate adsorbent surface.

3.4. Au(III) sorption, recovery and regeneration studies

The solution pH is one of the most important factors affecting the sorption process since the proton in acid solution can protonate binding sited of the ligand molecules, and hydroxide in the basic area may complex and precipitate many metal ions. In order to determine the optimum pH, the effect of pH on the complex formation and maximum sorption by the conjugate adsorbent were investigated over the range of 1.0–7.0, using hydrochloric acid or sodium hydroxide as indicated in experimental section. The Au(IIII) uptake was determined in different pH regions, and the results are depicted in **Fig. 6(A)**. The optimum pH for the uptake of Au(III) was an acidic condition at pH 3.50 as judged from **Fig. 6(A)**. The progressive decrease in sorption of Au(III) ions at low pH is due to competition of hydrogen ion with Au(IIII) for reaction with the DHDM immobilized conjugate adsorbent. It is also noted that ligand incorporated adsorbent has the specific sorption ability at the specific pH region for target metal ions [**29**].

The contact time is an important factor to achieve the highest sorption efficiency in determining the possibility of application of conjugate adsorbent for the selective recovery of Au(III) ions. In this work, different contact times were evaluated for the percentage of Au(III) sorption by conjugate adsorbent while the initial concentration was same in each case. The results are shown in **Fig. 6(B)**. The results also evident that Au(III) sorption versus time curves was single, smooth and continuous leading to saturation, suggesting the possible monolayer coverage of Au(III) ions on the conjugate adsorbent surface. The sorption efficiency increases with increasing time and exhibited a rapid sorption during the short contact time, followed by a slow increase until equilibrium was achieved. This two steps

sorption is reported by the ligand supported adsorbents [26]. It is noted that the rapid step is quantitatively predominant and probably due to the abundant availability of active sites on the conjugate adsorbent and the second step is slow and quantitatively insignificant with gradual occupancy of the pore surface active functional sites. The data also indicated that the equilibrium sorption was attained within 1 h. Then the contact of 3 h was assumed to be suitable for subsequent sorption experiments in this work for measuring the maximum sorption capacity by the conjugate adsorbent. However, biosorption and extraction are slow kinetics than the ion exchange and complexation mechanisms [32,33].

The maximum sorption studies were conducted by varying the initial Au(III) ions concentration while the adsorbent dose in each sample was kept identical. The Langmuir isotherm is based on the monolayer sorption on the active sites of the conjugate adsorbent. Based on Langmuir sorption theory, the sorption takes place at specific homogeneous sites on the conjugate adsorbent. Then the Langmuir sorption isotherm based on the assumption of all sorption sites are energetically same and sorption occurs on a structurally homogeneous conjugate adsorbent. The experimental sorption capacity and the sorption capacity predicted by the Langmuir are shown in **Fig. 7**. The Langmuir equation has been successfully applied to this sorption operation as follows:

$$C_e/q_e \ = \ 1/(K_L q_m) \ + \ (1/q_m)C_e \quad \text{(linear form)} \tag{5}$$

where q_m is the maximum sorption capacity, K_L is the Langmuir coefficient (L/mg), q_e is the amount of adsorbed Au(III) ions on conjugate adsorbent at equilibrium (mg/g) and C_e is the equilibrium liquid concentration (mg/L). Sorption isotherms (q_e versus C_e) showed that the sorption capacity, which is the mass (mg) of total Au(III) ions adsorbed per unit mass of adsorbent, increased with increasing equilibrium Au(III) ions concentration and eventually

16

attained a constant value (**Fig. 7**). The q_m and K_L are the Langmuir constants which are related to the sorption capacity and energy of sorption, respectively, and can be calculated from the intercept and slope of the linear plot, with C_e/q_e versus C_e as shown in **Fig. 7** (inset). The correlation coefficients value ($R^2=0.9941$) confirm that the Langmuir sorption equation can be considered an accurate model of the sorption behavior of the adsorbent. The maximum sorption capacity corresponding to complete monolayer coverage showed a mass capacity of 183.42 mg/g and the sorption coefficient K_L, which is related to the apparent energy of sorption, was calculated to be 1.91 L/mg.

The sorption capacity compared with literature values [**1,2,5,7,8,16,17,22,23**] listed in **Table 1**, the proposed conjugate adsorbent is found to be comparable and competitive with other forms of adsorbent materials. It was initially assumed that the higher maximum sorption capacity obtained for Au(III) by the conjugate adsorbent due to the spherical nanosized cavities with large surface area of the adsorbent would allow an increased equilibrium sorption capacity of Au(III) ions in optimum conditions. The differences of Au(III) uptake on various adsorbents are due to the properties of function groups, surface area and particle size of the adsorbents.

The presence of diverse metal ions affected the sorption affinity of Au(III). Then it is important to evaluate the sorption selectivity of the conjugate adsorbent to Au(III) ions. There are several cations co–existed such as Zn(II), Co(II), Fe(III), Ni(II), Cu(II), Ag(I), Bi(III), Pt(II), Ru(III), Pb(II) and Cr(III) in urban mining waste scrap with Au(III) ion. Therefore, multi–mixture ions solutions were chosen to investigate the sorption selectivity of conjugate adsorbent for Au(III). The results are depicted in **Fig. 8(A)**. The Au(III) was efficiently adsorbed by the conjugate adsorbent from the multi–mixture, and sorption percentage of Au(III) by the conjugate adsorbent was more than 97%, indicating that the adsorbent exhibited good sorption selectivity for Au(III). Therefore, it is confirmed that Au(III) ion has

17

high affinity to DHDM ligand incorporated conjugate adsorbent. Then it is expected that the conjugate adsorbent has potential applicability for recovery of Au(III) from urban mining waste in industrial electronic scrap.

An elution efficiency was evaluated in this study based on the ratio of the Au(III) extracted/recovered from the adsorbent to the Au(III) adsorbed onto the conjugate adsorbent. To investigate elution/recovery and reusability, sorption operations were performed according to the batch method. Then the adsorbent was saturated with Au(III) ion in the presence of competing ions and evaluate the exact eluent for complete recovery of Au(III) from the conjugate adsorbent. In treated with 2.0 M HCl, very low concentration of undesired metals ion was eluted while these were adsorbed during Au(III) sorption operation. The experimental data confirmed that 0.10 M thiourea–0.20 M HCl was suitable to recover the Au(III) ions from the adsorbent. **Scheme 2** shows the bonding mechanism of Au(III) with DHDM immobilized conjugate adsorbent and extraction/elution for next uses in optimum conditions. In elution operations, the conjugate adsorbent was simultaneously regenerated into the initial form without nanostructural damage of the adsorbent. The sorption capacity was calculated from the loading and elution tests. The reusability was also measured of each detection/sorption–elution cycles for ten cycles, and the sorption efficiency in each cycle was measured. The data clarified that the Au(III) sorption efficiency slightly decreased after ten cycles (**Fig. 8(B)**) indicating the many cycles uses for Au(III) recovery operations. Then the conjugate sorbent showed better long–term stability and reusability towards Au(III) ions.

4. Conclusions

The present study investigated the detection and recovery of ultra–trace Au(III) ions by solid–state conjugate adsorbent. The conjugate adsorbent was successfully prepared by *N*,*N*′–(octane–1,8–diylidene)di(2–hydroxy–3,5–dimethylaniline)　　　(DHDM)　　　ligand

immobilized onto inorganic mesoporous silica. The conjugate adsorbent was shown high selectivity to Au(III) even in the presence of diverse competing ions and able to accurate detection and recovery of ultra–trace Au(III) by naked–eye observation. The trace concentration level of Au(III) ions was determined due to charge transfer (intense π–π transition) between the functional groups of DHDM ligand molecule and Au(III) ions complexes. The equilibrium sorption data were well fitted with Langmuir isotherm model and confirmed the monolayer Au(III) sorption onto the conjugate adsorbent. The data clarified that the low of detection limit and maximum sorption capacity of the conjugate adsorbent were 0.22 µg/L and 183.42 mg/g, respectively. The Au(III) uptake was not affected by adding of common ions in sorption process and showed high selectivity performances even in the presence of high concentration competing ions. The adsorbed Au(III) was eluted with 0.10 M thiourea–0.20 M HCl eluent and regenerated into the initial form for next operation without significant deterioration in its original sorption performances. The reusability in multi cycles with high sorption capacity and stability of the adsorbent is implying the highly cost–effective for Au(III) detection and recovery from waste samples. Therefore, the Au(III) capturing in optically by conjugate adsorbent in nanoscale level led to new frontiers in nanoscience and nanotechnology. Based on the batch conditions and obtained results for Au(III) recovery, the conjugate adsorbent can be used as alternative adsorbent for ultra–trace Au(III) detection and recovery from urban mining waste.

References

[1] W. Nakbanpote, P. Thiravetyan, C. Kalambaheti, Minerals Engineering 15 (2002) 549.

[2] M. Laatikainen, E. Paatero, Hydrometallurgy 79 (2005) 154.

[3] Y. Zhao, Gold 27 (2006) 42.

[4] S. Changmei, Z. Guanghua, W. Chunhua, Q. Rongjun, Z. Ying, G. Quanyun, Chemical Engineering Journal 172 (2011) 713.

[5] H. Ebrahimzadeh, E. Moazzen, M.M. Amini, O. Sadeghi, Chemical Engineering Journal 215–216 (2013) 315.

[6] H. Ashkenani, M.A. Taher, Microchemical Journal 103 (2012) 185.

[7] M.R. Awual, M.A. Khaleque, M. Ferdows, A.M.S. Chowdhury, T. Yaita, Microchemical Journal 110 (2013) 591.

[8] L. Zhang, Z. Li, Z. Hu, X. Chang, Spectrochimica Acta Part A 79 (2011) 1234.

[9] A.S. Amin, Spectrochimica Acta Part A 77 (2010) 1054.

[10] I. Jarvis, M.M. Totland, K.E. Jarvis, Analyst 122 (1997) 19.

[11] L. Elci, D. Sahan, A. Basaran, M. Soylak, Environmental Monitoring and Assessment 132 (2007) 331–338.

[12] M. Iglesias, E. Anticy, V. Salvady, Analytica Chimica Acta 381 (1999) 61–67.

[13] P. Liang, E. Zhao, Q. Ding, D. Du, Spectrochimica Acta B 63 (2008) 714.

[14] S. Chen, X. Zhu, Minerals Engineering 23 (2010) 1152.

[15] S. Sen, A. Seyrankaya, Y. Cilingir, Minerals Engineering 18 (2005) 1086.

[16] T. Kinoshita, Y. Ishigaki, K. Nakano, K. Yamaguchi, S. Akita, S.Nii, F. Kawaizumi, Separation and Purification Technology 49 (2006) 253.

[17] M. Soleimani, T. Kaghazchi, Journal of Industrial and Engineering Chemistry 14 (2008) 28.

[18] M. Tuzen, K.O. Saygi, M. Soylak, Journal of Hazardous Materials 156 (2008) 591–595.

[19] L. Tavakoli, Y. Yamini, H. Ebrahimzadeh, A. Nezhadali, Sh. Shariati, F. Nourmohammadian, Journal of Hazardous Materials 152 (2008) 737–743.

[20] R. Qu, C. Sun, M. Wang, C. Ji, Q. Xu, Y. Zhang, C. Wang, H. Chen, P. Yin, Hydrometallurgy 100 (2009) 65–71.

[21] E. Ertan, M. Gulfen, Journal of Applied Polymer Science 111 (2009) 2798.

[22] H. Koyanaka, K. Takeuchi, C.K. Loong, Separation and Purification Technology 43 (2005) 9.

[23] C.P. Gomes, M.F. Almeida, J.M. Loureiro, Gold recovery with ion exchange used resins, Separation and Purification Technology 24 (2001) 35.

[24] J.M. Sanchez, M. Hidalgo, V. Salvado, Reactive and Functional Polymers 49 (2001) 215.

[25] P. Liu, Q. Pu, Z. Su, Analyst 125 (2000) 147.

[26] (a) M.R. Awual, T. Yaita, H. Shiwaku, Chemical Engineering Journal 228 (2013) 327; (b) M.R. Awual, T. Kobayashi, Y. Miyazaki, R. Motokawa, H. Shiwaku, S. Suzuki, Y. Okamoto, T. Yaita, Journal of Hazardous Materials 252–253 (2013) 313; (c) M.R. Awual, T. Kobayashi, Y. Miyazaki, R. Motokawa, H. Shiwaku, S. Suzuki, Y. Okamoto, T. Yaita, Chemical Engineering Journal 225 (2013) 558.

[27] (a) M.R. Awual, T. Yaita, S.A. El–Safty, H. Shiwaku, Y. Okamoto, S. Suzuki, Chemical Engineering Journal 222 (2013) 172; (b) M.R. Awual, M. Ismael, T. Yaita, S.A. El–Safty, H. Shiwaku, Y. Okamoto, S. Suzuki, Chemical Engineering Journal 222 (2013) 67; (c) M.R. Awual, M. Ismael, M.A. Khaleque, T. Yaita, Journal of Industrial and Engineering Chemistry (2013) http://dx.doi.org/10.1016/j.jiec.2013.10.009.

[28] (a) M.R. Awual, T. Yaita, S.A. El–Safty, H. Shiwaku, S. Suzuki, Y. Okamoto, Chemical Engineering Journal 221 (2013) 322; (b) M.R. Awual, T. Yaita, Sensors and Actuators B: Chemical 183 (2013) 332.

[29] (b) M.R. Awual, I.M.M. Rahman, T. Yaita, M.A. Khaleque, M. Ferdows, Chemical Engineering Journal 236 (2014) 100; (d) M.R. Awual, M. Ismael, T. Yaita, Sensors and Actuators B 191 (2014) 9.

[30] G.S. Attard, J.C. Glyde, C.G. Goltner, Nature 378 (1995) 366.

[31] H. Dai, J. Yang, J. Ma, F. Chen, Z. Fei, M. Zhong, Microporous and Mesoporous Materials 147 (2012) 281.

[32] (a) M.R. Awual, A. Jyo, T. Ihara, N. Seko, M. Tamada, K.T. Lim, Water Research 45 (2011) 4592; (b) M.R. Awual, A. Jyo, Desalination 281 (2011) 111; (c) M.R. Awual, A. Jyo, Water Research 43 (2009) 1229; (d) M.R. Awual, A. Jyo, S.A. El–Safty, M. Tamada, N. Seko, Journal of Hazardous Materials 188 (2011) 164; (e) M.R. Awual, M.A. Shenashen, A. Jyo, H. Shiwaku, T. Yaita, Journal of Industrial and Engineering Chemistry (2013) http://dx.doi.org/10.1016/j.jiec.2013.11.016.

[33] (a) M.R. Awual, S. Urata, A. Jyo, M. Tamada, A. Katakai, Water Research 42 (2008) 689; (b) M.R. Awual, M.A. Shenashen, T. Yaita, H. Shiwaku, A. Jyo, Water Research 46 (2012) 5541; (c) M.R. Awual, S.A. El–Safty, A. Jyo, Journal of Environmental. Sciences 23 (2011) 1947; (d) M.R. Awual, M.A. Hossain, M.A. Shenashen, T. Yaita, S. Suzuki, A. Jyo, Environmental Science and Pollution Research 20 (2013) 421.

Table 1

Comparison of sorption capacities towards Au(III) by using various materials.

Used adsorbents	Capacity (mg/g)	Ref.
HSAS	30.21	[17]
Activated carbon	35.88	[1]
Attapulgite	66.70	[8]
IIP@MWCNTs	67.00	[5]
Mn_2O_3 adsorbent,	70.00	[22]
XAD–7	98.48	[2]
Purolite A–100	111.5	[23]
PEGDA	121.0	[16]
Mesoporous adsorbent	177.94	[7]
Conjugate adsorbent	183.42	This study
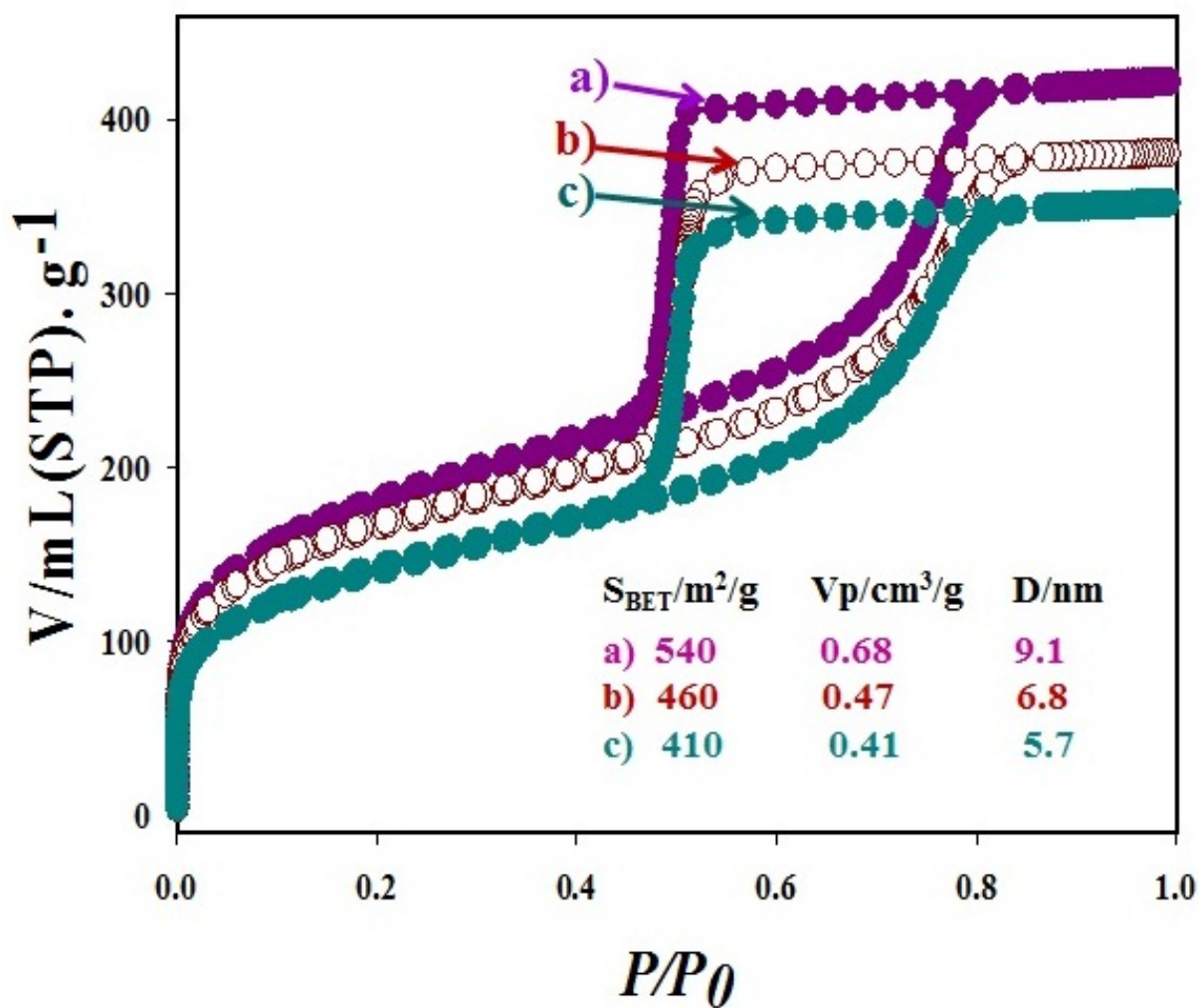
Fig. 1. N$_2$ adsorption/desorption isotherms at 77 K of (a) inorganic mesoporous silica synthesized by using direct templating method, (b) conjugate adsorbent and (c) conjugate adsorbent after Au(III) sorption with the difference of surface areas, pore sizes and volumes.
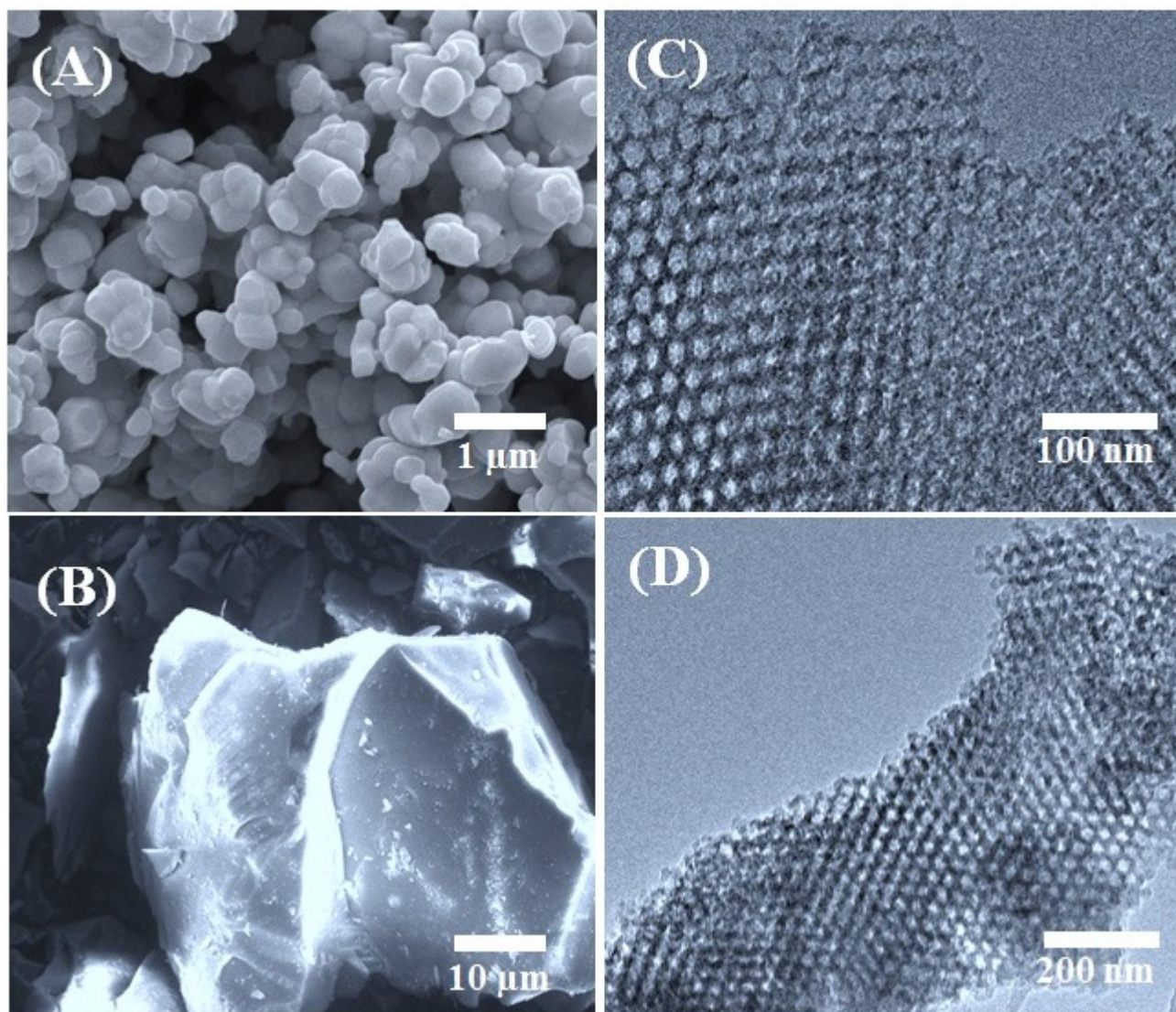
Fig. 2. SEM images of the inorganic mesoporous silica monoliths prepared by instant direct–templating method (A, B); TEM images representative of ordered structures along with uniformly pores in all directions (C, D).
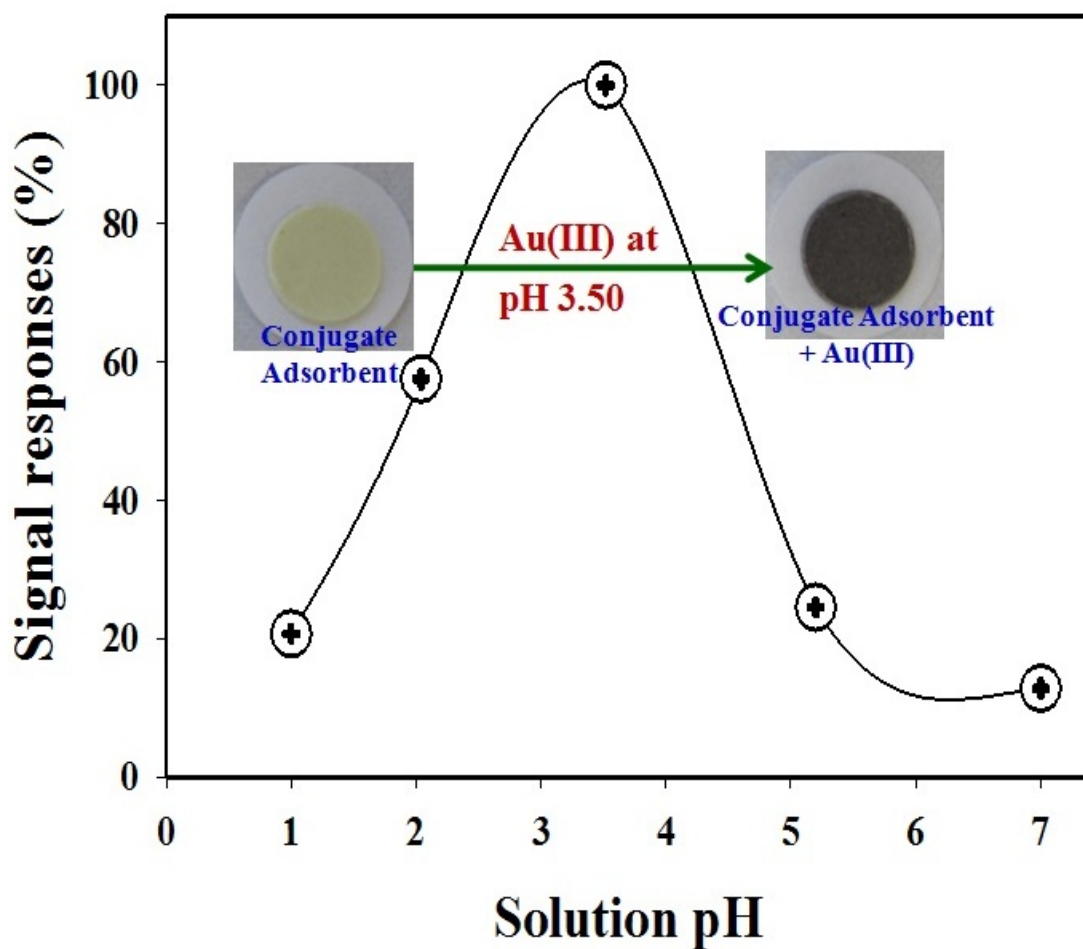
Fig. 3. Effect of pH for ultra–trace Au(III) detection by conjugate adsorbent. The equilibrated individually at different pH conditions with 2.0 mg/L of Au(III) ions at 25°C in 10 mL volume for 10 min. The standard deviation was >2.5% for the analytical data of duplicate analyses.
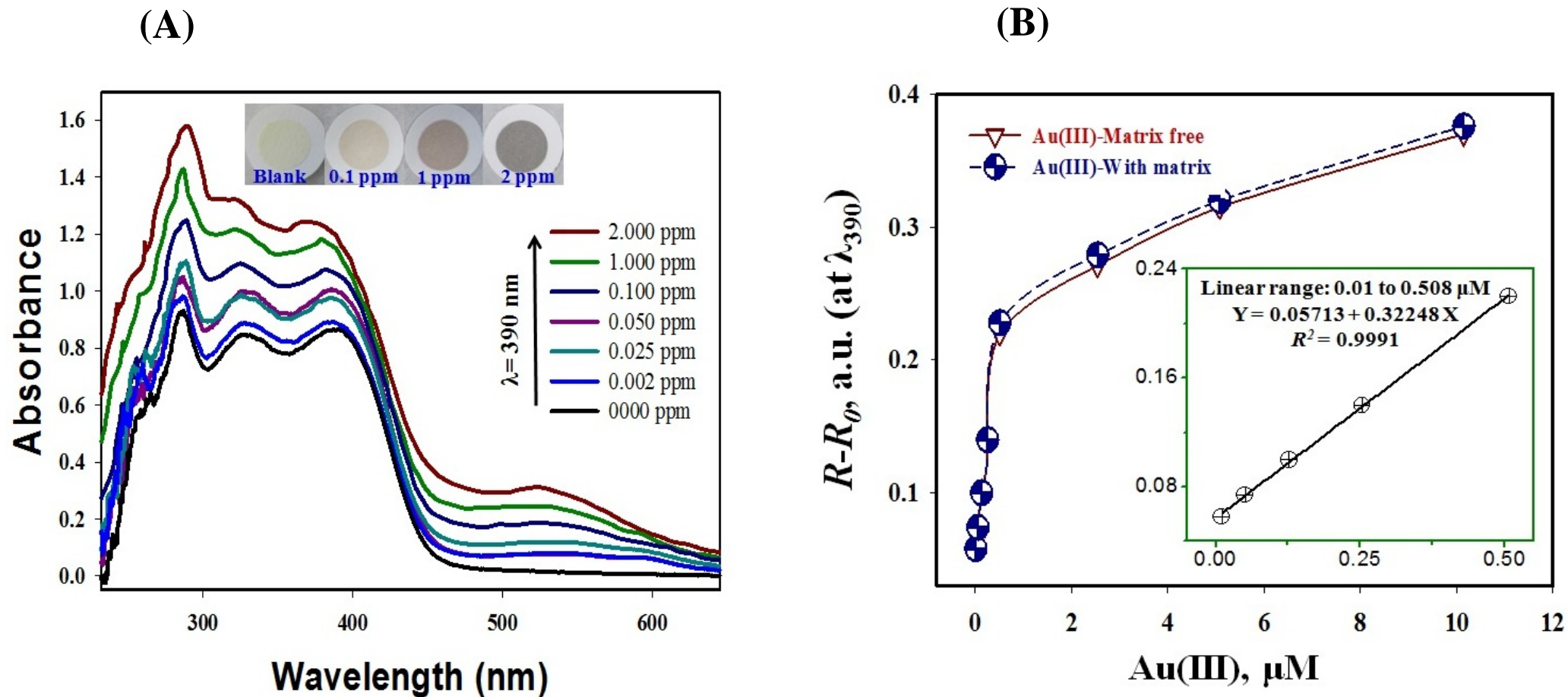
Fig. 4. (A) The color optimization at different Au(III) concentrations corresponds to the absorbance spectral intensity and (B) calibration profile with spectral absorbance measured at 390 nm with Au(III) ion concentrations. The inlets in graphs (B) show the low–limit of detection with a linear fit in the linear concentration range. The R and R_0 are the absorbance signal responses of the adsorbent after and before addition of Au(III) ion. The dotted line represents the calibration plot of the Au(III) ions in the presence of active interfering species under the same determination conditions. The error bars denote a relative standard deviation of $\geq 3\%$ range for the analytical data of 4 replicates analyses.
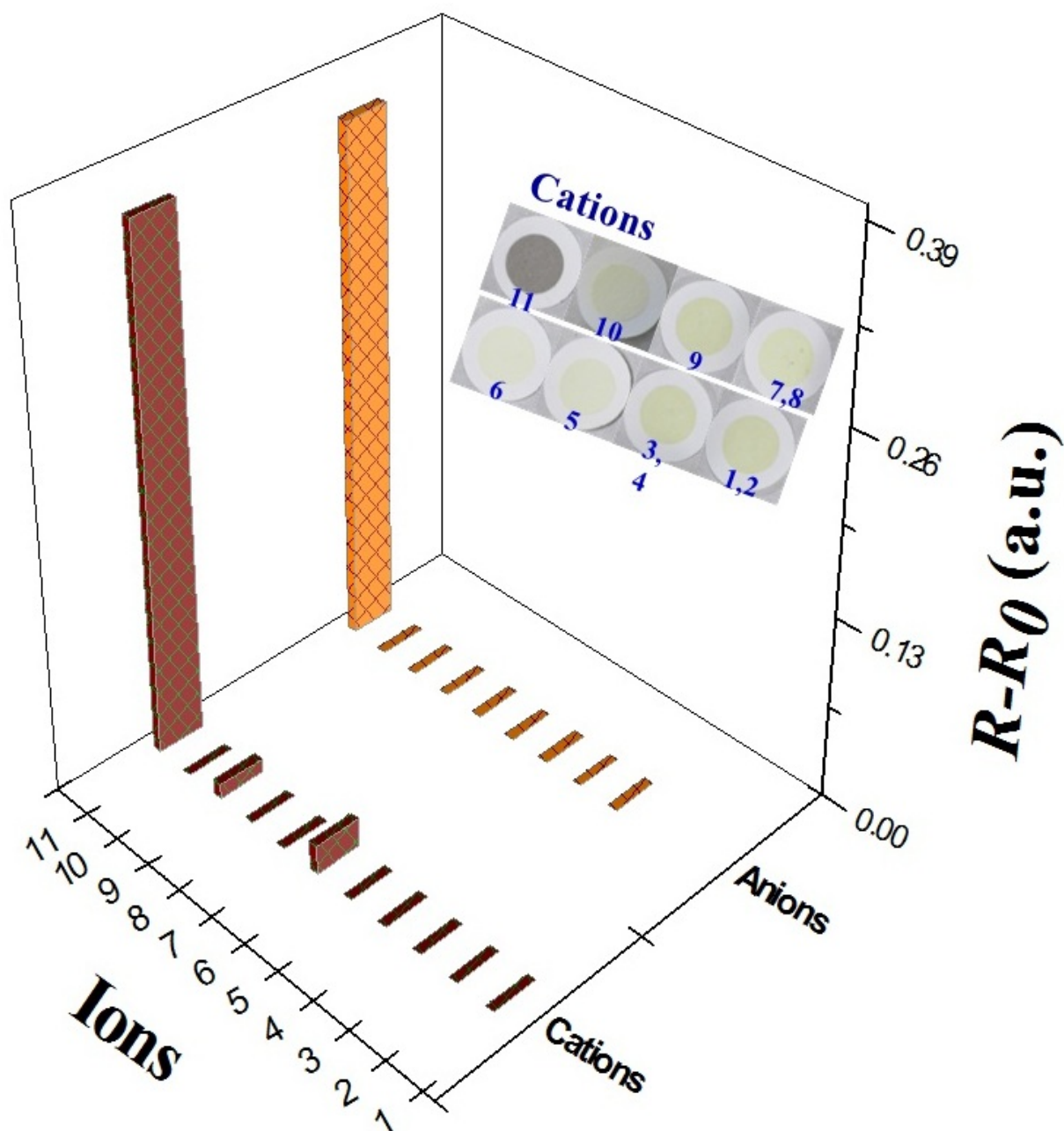
Fig. 5. Ion selectivity profiles of the conjugate adsorbent after adding different metal ions at optimal conditions. The interfering cations (10.0 mg/L) are listed in order (1 to 11): (1) Zn^{2+}, (2) Fe^{3+}, (3) Bi^{3+}, (4) Pt^{2+}, (5) Ru^{3+}, (6) Ag^+, (7) Ni^{2+}, (8) Cu^{2+}, (9) Co^{2+}, (10) Blank and (12) 2.0 ppm Au^{3+}. The interfering (500 mg/L) anions are listed in order (3 to 9): (3) chloride, (4) nitrate, (5) sulfate, (6) phosphate, (7) bicarbonate, (8) carbonate and (9) citrate.
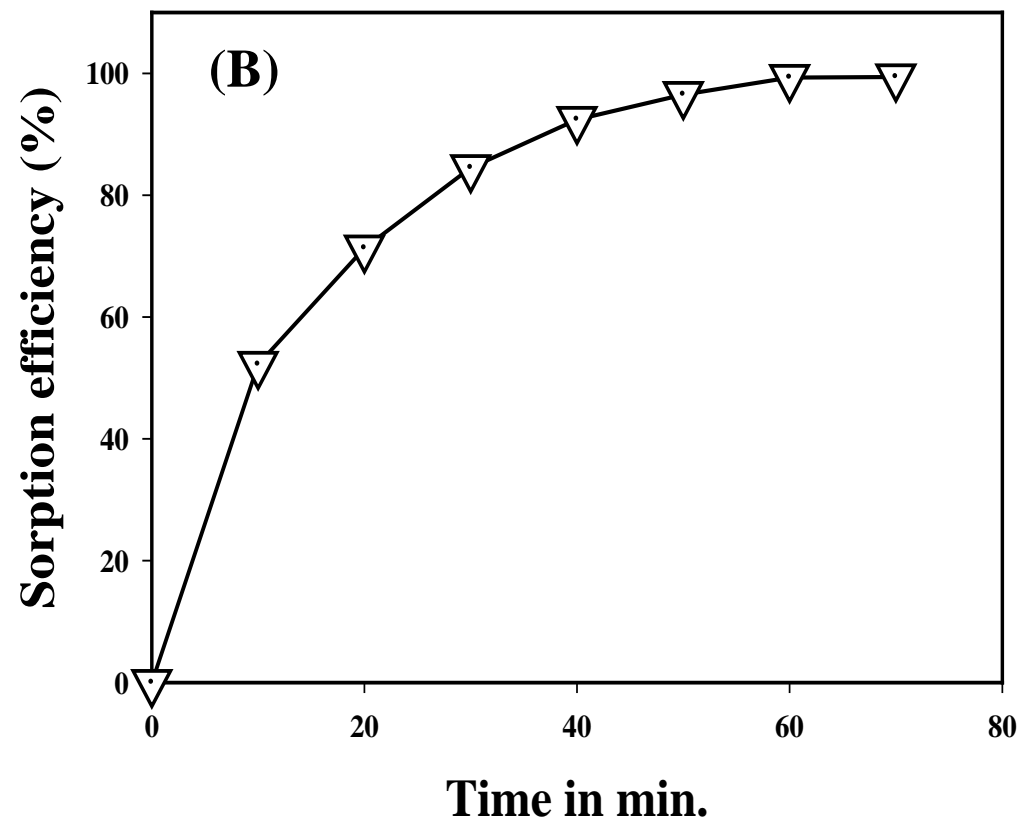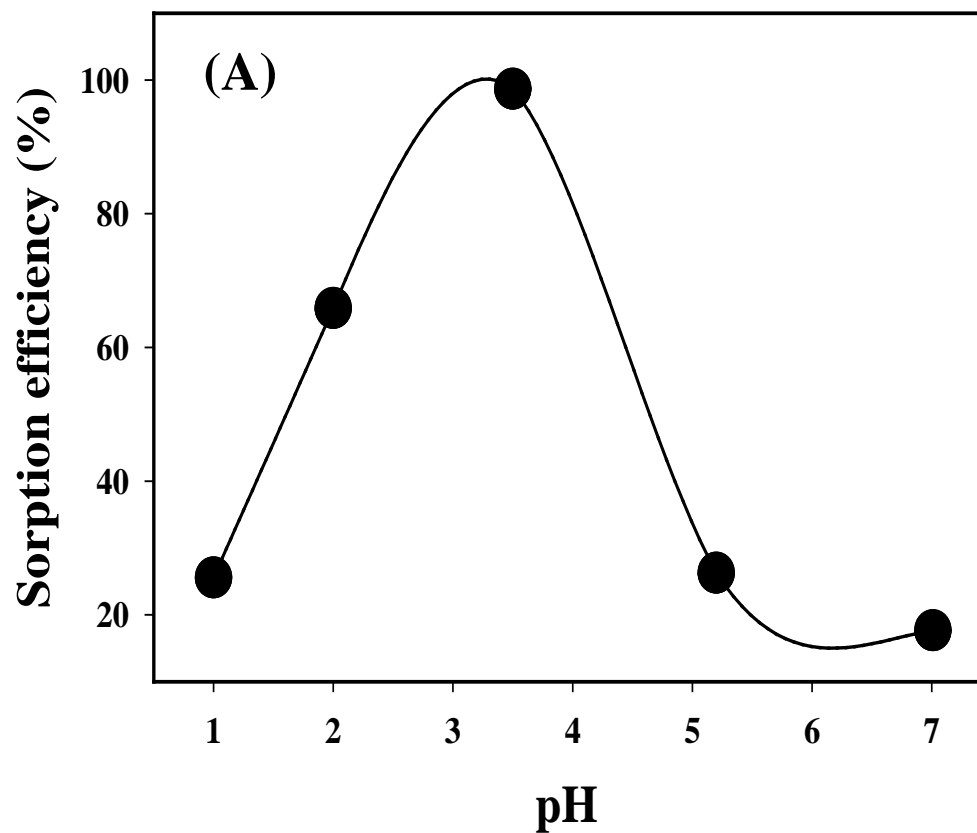
Fig. 6. (A) Sorption of Au(III) ions by the conjugate adsorbent under different pH regions; (B) equilibrium contact time for maximum Au(III) ions sorption when Au(III) concentration was 5.0 mg/ in 20 mL. The RSD value was ~3.5%.
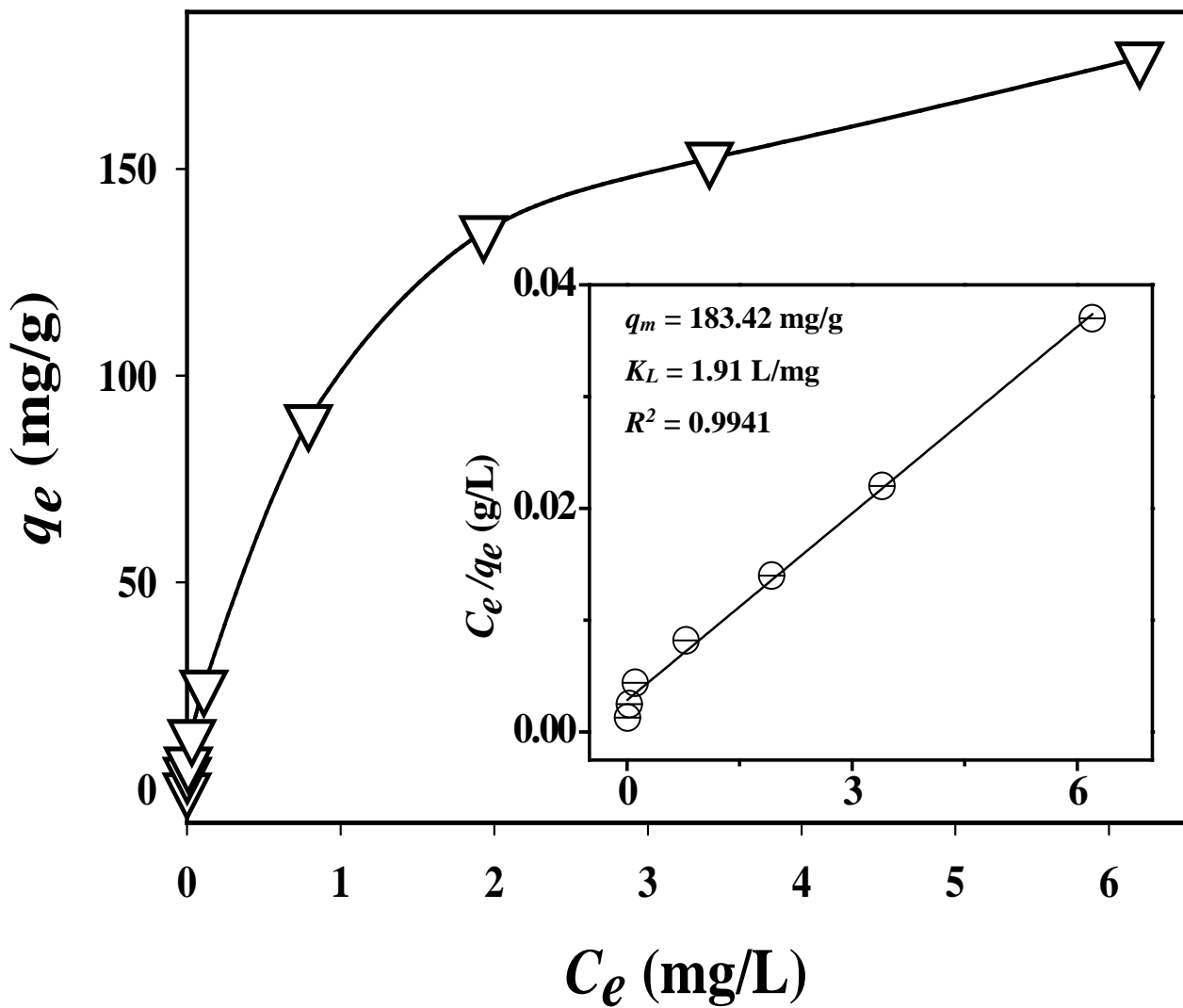
Fig. 7. Langmuir sorption isotherms of Au(III) ions and the linear form of the Langmuir plot (initial Au(III) ion concentration range 1.02 – 80.16 mg/L; solution pH 3.50; dose amount 8 mg; solution volume 20 mL and contact time 3 h).
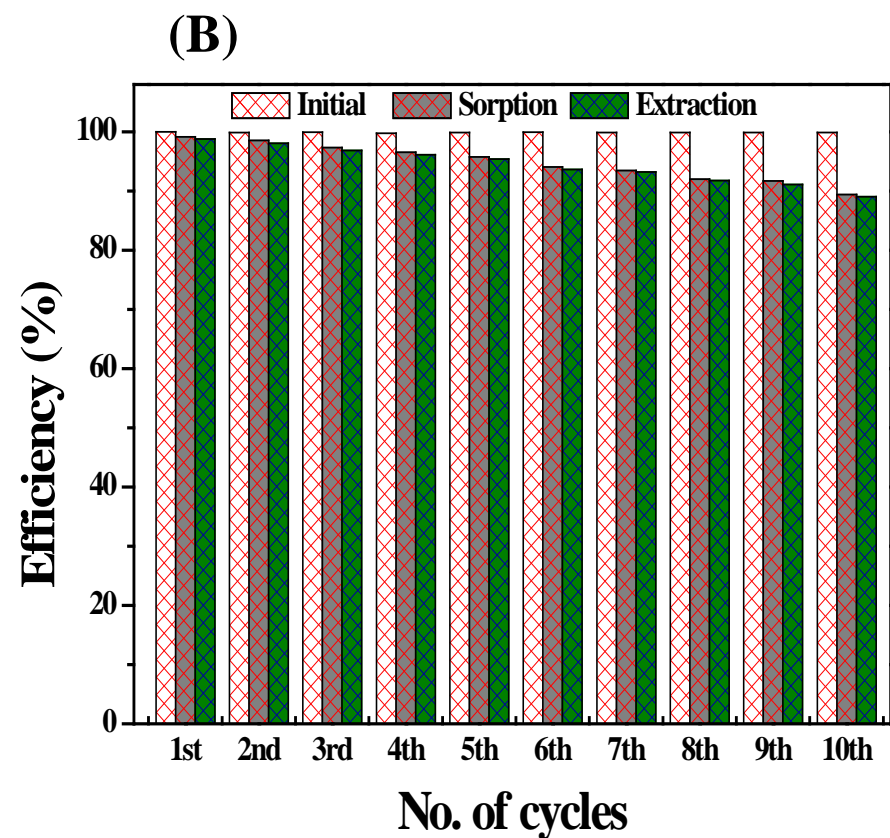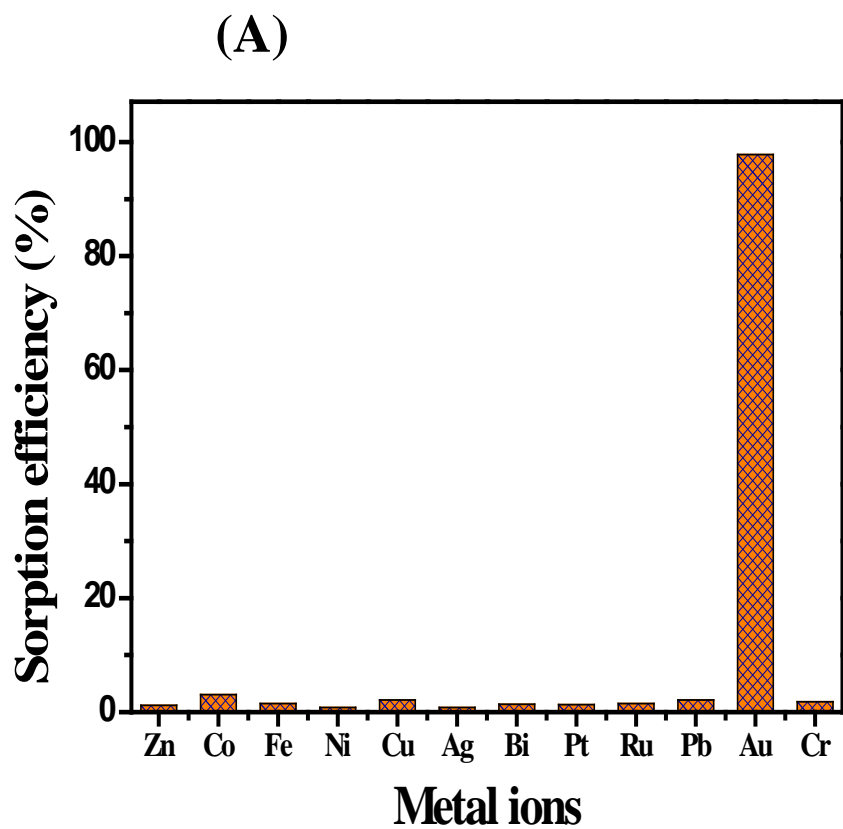
Fig. 8. (A) The Au(III) sorption in the presence of competitive multi–metal ions from the solutions by the novel conjugate adsorbent. The competing ions concentration was 10 mg/L and Au(III) concentration was 2.0 mg/L; (B) ICP–AES analysis of Au(III) ions after completing sorption and extraction within ten cycles. The RSD values were ~4.0%.
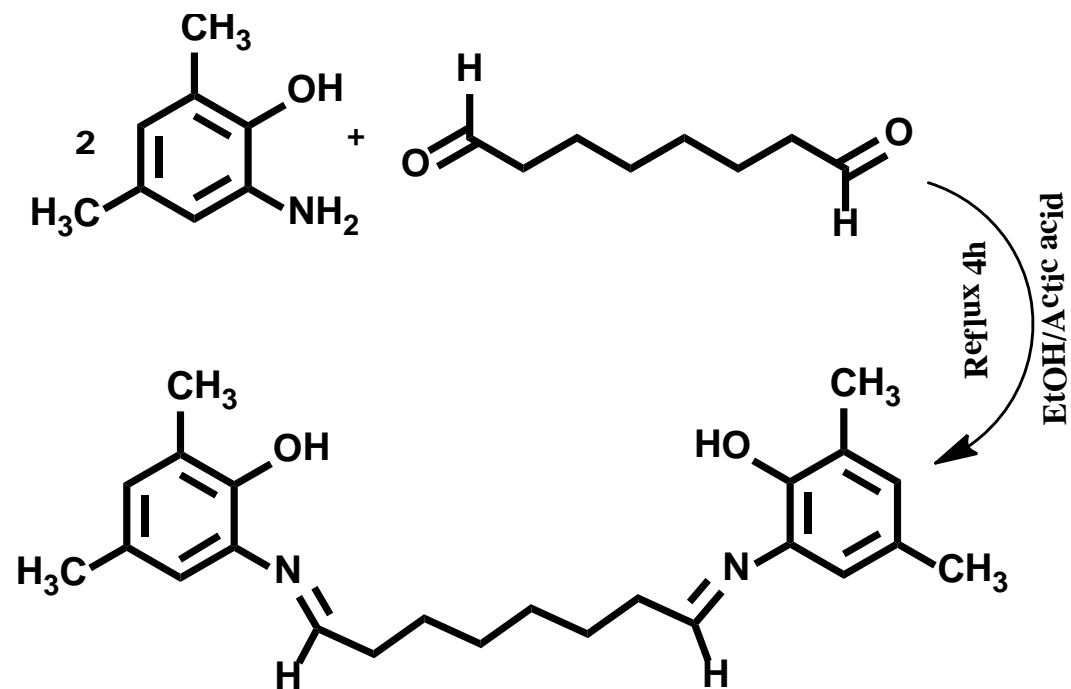
Scheme 1. Preparation steps and structure of *N,N′*–(octane–1,8–diylidene)di(2–hydroxy–3,5–dimethylaniline) (DHDM) ligand.
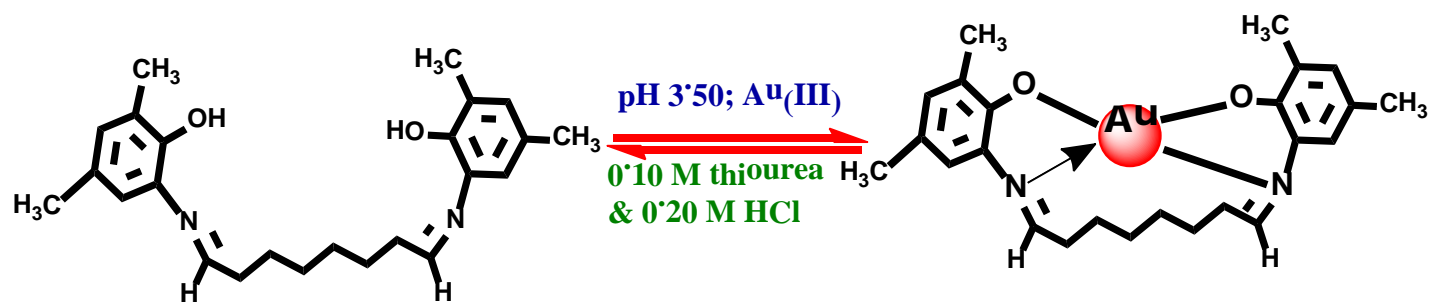
Scheme 2. The possible complexation mechanism of Au(III) and DHDM at pH 3.50 during detection and sorption operation and complete recovery of Au(III) with suitable eluent of 0.10 M thiourea–0.20 M HCl.

33